2012 IEEE International Conference on Robotics and Automation
RiverCentre, Saint Paul, Minnesota, USA
May 14-18, 2012

# Object motion–decoupled internal force control for a compliant multifingered hand

Domenico Prattichizzo, Monica Malvezzi, Marco Aggravi and Thomas Wimböck

*Abstract*— **Compliance in multifingered hand improves grasp stability and effectiveness of the manipulation tasks. Compliance of robotic hands depends mainly on the joint control parameters, on the mechanical design of the hand, as joint passive springs, and on the contact properties. In object grasping the primary task of the robotic hand is the control of internal forces which allows to satisfy the contact constraints and consequently to guarantee a stable grasp of the object. When compliance is an essential element of the multifingered hand, and the control of the internal forces is not designed to be decoupled from the object motion, it happens that a change in the internal forces causes the object trajectory to deviate from the planned path with consequent performance degradation. This paper studies the structural conditions to design an internal force controller decoupled from object motions. The analysis is constructive and a controller of internal forces is proposed. We will refer to this controller as object motion-decoupled control of internal forces. The force controller has been successfully tested on a realistic model of the DLR Hand II. This controller provides a trajectory interface allowing to vary the internal forces (and to specify object motions) of an underactuated hand, which can be used by higher-level modules, e.g. planning tools.**

## I. INTRODUCTION

In multifingered robotic hands, compliance can be present at the joint level as part of the mechanical design with passive springs, at the joint control and at the contacts due to soft finger pads or to deformable objects. For a complete geometrical characterization of compliance refer to [9] where the authors consider also the effects on compliance due to small changes in grasp geometry.

Compliance is essential in robotic grasping when high precision is required as in assembling tasks [9]. Compliance plays a key role in hand design when robustness and dependability are required for human robot interaction as discussed in [1] where the concept of soft robotics is introduced. Compliance introduced through passive mechanical adaptation is assuming a great importance also in underactuated robotics which refers to systems having more DoFs than actuators. One of the commonly used approaches in underactuated multifingered hands is to introduce springs to adapt to various object geometries in a simple and robust way [6], [8], [10], [11]. The use of soft fingertips is proposed in [2] to generate variable stiffness for a grasp by modification of the internal grasp forces. The compensation of the object displacement, however, was not deeply studied.

There is another reason to explicitly consider stiffness: in grasp configurations, as in power grasp, where the number of degrees of freedom (DoF) of the hand is lower than dimension of the contact force vectors, compliance at the contact points allows to solve the problem of force distribution, which becomes statically indeterminate.

D. Prattichizzo is with Department of Information Engineering, University of Siena, Italy, and with Department of Advanced Robotics, Istituto Italiano di Tecnologia, Genova, Italy prattichizzo@dii.unisi.it
M. Malvezzi and M. Aggravi are with Department of Information Engineering, University of Siena, Italy malvezzi@dii.unisi.it, aggravi@dii.unisi.it
T. Wimböck is with DLR German Aerospace Center Institute of Robotics and Mechatronics, Germany Thomas.Wimboeck@dlr.de

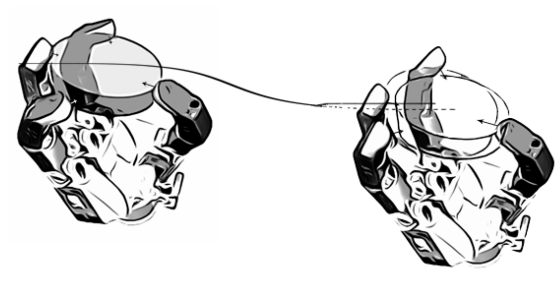

Fig. 1. The effect on object trajectory caused by an internal force controller that does not explicitly consider the decoupling from the object motion.

The main issue when compliance is not negligible is that controlling robotic multifingered hands corresponds to trade-off between the required level of safety, in terms of grasp stability and robustness, and the level of performances [1]. The compliance strongly couples the force distribution at the contacts and the hand configuration making difficult to reliably and independently control both the contact forces and the object trajectory.

The problem we consider in this paper deals with control of compliant multifingered hands and refers to performance of the internal force controller. Consider Fig. 1 and assume that the hand is grasping an object and is tracking a given object trajectory as in the left part of the figure. At a certain point there are increased object forces expected. However, the controller of internal force does not explicitly takes into account the object motion, in other terms it is not decoupled from the object motion control, and moves the object of about six millimetres in an undesired direction, as shown in the right part of the figure. The robotic hand applies more internal force but ends to track a trajectory, the dashed one, different from the planned one. This error in the trajectory tracking is due to the compliance of the robotic hand and to the fact that the internal controller is not explicitly designed to compensate for such undesired motion.

Note that the undesired and uncontrolled change displacement of the object is very dangerous in all tasks where the position accuracy is important as in medical applications. This paper contributes to solve this issue proposing an internal force controller which is decoupled from the motion of the grasped object.

This work builds upon previous contribution [12] where preliminary results on the internal force controller are presented. Based on our previous work, in which the quasi-static mappings were derived and examined, the contribution of this paper consists of proposing a controller which takes the set point for - what we term - the *object motion-decoupled control of internal forces*. The proposed controller gives the setpoints for a position controlled robot hand that has passive joint compliance.

We therefore extend the previous work by applying the new controller to the hand object dynamics of a compliant dexterous robotic hand and evaluate its performance by means of numerical experiments.

The paper is organized as follows: Section II summarizes the quasi-static and kinematic equations that describes hand grasping, the subspaces of controllable internal forces and rigid body motions are identified. Section III define which controllable internal forces can be produced without changing grasped object position. Section IV shows an application of the results theoretically identified in Section III on the dynamic model of the DLR Hand II [7]. Section V discusses and summarizes the obtained results.

## II. INTERNAL FORCE AND OBJECT MOTION IN GRASPING

### A. Static equilibrium equations

The equilibrium, congruence and constitutive equations necessary for a compliant multifingered hand grasping an object are here summarized. Further details can be found in [12]. The force and moment balance for the object are described by the equation

$$w = -G\lambda \tag{1}$$

where $w \in \Re^6$ is the external load wrench applied to the object; $\lambda \in \Re^{n_l}$ is the contact force vector in stacked notation, whose dimension $n_l$ depends both on the contact model and on the number of contact points; $G \in \Re^{6\times n_l}$ is the grasp matrix. For a complete definition of the grasp matrix along with the contact models, the reader is referred to [16]. The solution for the contact forces can be expressed as

$$\lambda = -G^{\#}w + A\mu$$

where $G^{\#}$ is the pseudoinverse of grasp matrix, $A \in \Re^{n_l\times h}$ is a matrix whose columns form a basis for the nullspace of $G$ ($\ker(G)$) and $\mu \in \Re^h$ is a vector that parametrizes the homogeneous part of the solution to (1). The generic homogeneous solution $\lambda_o = A\mu$, represents a set of contact forces whose resultant force and moment are zero. The contact forces included in the nullspace of $G$ are referred to as internal forces.

Internal forces are paramount in grasp control. In force-closure grasps, a convenient control of internal forces guarantees that the whole vector of forces complies with contact friction constraints notwithstanding disturbances acting on the manipulated object.

Not all the internal forces can be arbitrarily controlled by the hand, in order to define the subset of controllable internal forces the hand actuation has to be considered. The relationship between hand joint torques $\tau \in \Re^{n_q}$, where $n_q$ is the number of actuated joints, and contact forces is

$$\tau = J^{\mathrm{T}}\lambda \tag{2}$$

where $J \in \Re^{n_l\times n_q}$ is the hand Jacobian matrix [16]. We observe that in general the problem is not invertible and thus the contact forces $\lambda$ cannot be arbitrarily controlled acting on joint torques $\tau$.

The nullspaces of matrices $J$ and $G$ and their transposes have a relevant influence on the behaviour of the manipulation system. For a complete analysis of these subspaces on the grasp properties refer to [16] and therein references. If the intersection between the null space of $J^{\mathrm{T}}$ and the null space of $G$ is not trivial, the system composed of (1) and (2) results to be statically indeterminate (hyperstatic). In other terms it does not admit a unique solution. To solve the problem of force distribution in this case we need to introduce other equations, usually referred to as constitutive equations, that model the system compliance.

### B. Contacts and hand joints compliance

According to the procedure described in [3], consider an equilibrium starting configuration, in which the hand, in the configuration $q_0$, is grasping an object on which the external load $w_0$ is applied, by the contact forces $\lambda_0$. The contact force variation is expressed as follows

$$\delta\lambda = K_s(\delta c^h - \delta c^o) \tag{3}$$

where $\delta c^h \in \Re^{n_l}$ and $\delta c^o \in \Re^{n_l}$ are the displacements of the contact points on the hand and on the object respectively, while $K_s \in \Re^{n_l\times n_l}$ represents the contact stiffness matrix. The contact point displacement on the hand can be related to joint variable variation $\delta q$ as

$$\delta c^h = J\delta q \tag{4}$$

and contact point displacement on the object can be related to object displacement $\delta u$: [1]

$$\delta c^o = G^{\mathrm{T}}\delta u \tag{5}$$

Eq. (3) can be rewritten in terms of compliance, taking into account the kinematic relationships (4) and (5) as

$$C_s\delta\lambda = J\delta q - G^{\mathrm{T}}\delta u$$

where $C_s = K_s^{-1} \in \Re^{n_l\times n_l}$ represents the contact compliance. Consider the hand joints and assume that they are impedance controlled with joint stiffness $K_q \in \Re^{n_q\times n_q}$. The joint torques are proportional to the difference between the reference values of the joint variables, $q_r$, and their actual values $q$ and in terms of variations we can write

$$\delta\tau = K_q(\delta q_r - \delta q)$$

or

$$C_q\delta\tau = (\delta q_r - \delta q)$$

where $C_q = K_q^{-1} \in \Re^{n_q\times n_q}$ is the joint compliance.

### C. Internal forces

From (2) consider a small variation with respect to the reference equilibrium conditions. According to differentiation rules, the following relationship between joint torque and contact force variations can be computed (see [12])

$$\delta\lambda = K\left(J_r\delta q_r - G^{\mathrm{T}}\delta u\right) \tag{6}$$

where

$$K = \left(C_s + J_rC_qJ^{\mathrm{T}}\right)^{-1} \quad J_r = J\left(I + C_qT\right) \quad T = \frac{\partial J^{\mathrm{T}}\lambda}{\partial q}$$

[1] The object position and orientation is here defined by a vector $u \in \Re^6$, defined as $u = [p^{\mathrm{T}}\ \ \phi^{\mathrm{T}}]^{\mathrm{T}}$, where $p \in \Re^3$ denotes the position of the origin of the object reference frame with respect to the base one (usually on the hand palm), while $\phi \in \Re^3$ represents the orientation of the object reference frame with respect to the base one, represented here by the Euler angles.

Contact forces in (6) are those forces generated by joint reference variation $\delta q_r$ and object displacement $\delta u$ in a quasi-static setting. In what follows we are interested in evaluating the new equilibrium configuration that the system reaches when the joint reference changes by a term $\delta q_r$. In particular, the contact force variation $\delta\lambda$ and the object displacement $\delta u$.

It is worth underlying that all contact forces variations in (6) are internal in the sense that they are balanced, since the external load $w$ applied to the object is considered constant.

In this paper we are interested in particular to evaluate the effect on the internal forces (6) due to actions on the joint reference only. In other terms we will evaluate those internal force that are controllable by changes of the joint reference $\delta q_r$ only.

The problem of computing the controllable internal forces has been solved evaluating, from this initial equilibrium condition, the variations of the joint reference variable $\delta q_r$ and studying the new equilibrium condition.

By differentiating (1) and assuming that the external load $w_0$ is constant, we obtain

$$0 = -G\delta\lambda + N\delta u, \quad N = -\frac{\partial G\lambda}{\partial u} \tag{7}$$

where $N$ takes into account the variation of the grasp matrix elements in the new equilibrium configuration. This term can be neglected only if the grasp matrix is constant and/or the contact forces in the reference configuration are small. By substituting expression (6) in (7), we can express the object motion $\delta u$ as a function of the joint reference variation $\delta q_r$ as

$$\delta u = \left(GKG^{\mathrm{T}} + N\right)^{-1} GKJ_r\delta q_r = V\delta q_r$$

and the corresponding contact force variation

$$\delta\lambda_c = \left(I - KG^{\mathrm{T}}\left(GKG^{\mathrm{T}} + N\right)^{-1} G\right) KJ_r\delta q_r = P\delta q_r$$

as a function of the joint reference variable change $\delta q_r$.

Define $E \in \Re^{n_l \times e}$ as a basis matrix of the column space of matrix $P$, the generic controllable internal force can be expressed as

$$\delta\lambda_c = Ey$$

where $y \in \Re^e$ is the generic vector that parametrizes the controllable contact forces.

### D. Rigid object motion

Rigid-body kinematics are of particular interest in the control of manipulation systems. They do not involve virtual contact spring deformations, thus they can be regarded as low-energy motions. In fact, rigid-body kinematics represent the easiest way to move the object.

Furthermore, if we impose a rigid body motion to the system, the internal forces do not change. So, when the internal forces are controlled by the joint actuators, we could use the rigid body motion to recover, in some way, the object displacement.

Rigid-body kinematics has been studied in a quasi-static setting in [3], [4] and in terms of unobservable subspaces from contact forces in [14], [15]. In [5] the problem has been analysed also in presence of passive joints.

According to (6), a rigid body motion, i.e. a system displacement that does not involve variation in the contact forces, can be evaluated as a solution of the homogeneous system:

$$J_r\delta q_r - G^{\mathrm{T}}\delta u = 0, \quad \begin{bmatrix} J_r & -G^{\mathrm{T}} \end{bmatrix} \begin{bmatrix} \delta q_r \\ \delta u \end{bmatrix} = 0$$

Rigid kinematics can then be described by a matrix $\Gamma$ whose columns form a basis for $\ker\begin{bmatrix} J_r & -G^{\mathrm{T}} \end{bmatrix} = \mathrm{im}(\Gamma)$. The generic solution of the system (II-D) can be expressed as:

$$\begin{bmatrix} \delta q_r \\ \delta u \end{bmatrix} = \Gamma x$$

The matrix $\Gamma$ can be partitioned as follows:

$$\Gamma = \begin{bmatrix} \Gamma_r & \Gamma_{qc} & 0 \\ 0 & \Gamma_{uc} & \Gamma_i \end{bmatrix}$$

where $\Gamma_r$ a basis matrix of the subspace of redundant manipulator motions $\ker(J_r)$, $\Gamma_i$ a basis matrix of the subspace of indeterminate object motions $\ker(G^T)$, and $\Gamma_{qc}$ and $\Gamma_{uc}$ conformal partitions of a complementary basis matrix It is evident that $J_r\Gamma_{qc} = G^T\Gamma_{uc}$.

The column space of $\Gamma_c = \begin{bmatrix} \Gamma_{qc} \\ \Gamma_{uc} \end{bmatrix}$ consists of coordinated rigid-body motions of the mechanism, for the manipulator ($\Gamma_{qc}$) and the object ($\Gamma_{uc}$) components. As highlighted before, physically, rigid-body displacements do not involve variation of contact forces.

In [15], it has been shown that rigid-body motions are controllable, i.e. they belong to the space of controllability of the linear system that represents the dynamics of the system, with input the vector of joint generalized forces $\tau$. Note that the rigid-body subspace is only a subspace of the reproducible motions which also contains motions due to deformations of elastic elements in the model [3].

## III. Internal force control decoupled from object motions

Given a generic object motion that belongs to the rigid body motion subspace, i.e.

$$\delta u_{rb} = \Gamma_{uc}\beta,$$

the corresponding set of joint displacements can be evaluated as

$$\delta q_{rb} = V^{\#}\delta u_{rb} + Q\mu$$

where $V^{\#}$ denotes the pseudoinverse of $V$, $Q$ is a matrix whose columns form a basis of the nullspace of $V$, $\mu$ is an arbitrary vector whose length is given by the dimension of $V$ nullspace. The corresponding internal forces that can be generated is

$$\delta\lambda_c = PV^{\#}\Gamma_{uc}\beta + PQ\mu. \tag{8}$$

Internal force vector (8) belongs to the subspace of internal forces controllable and compensable: controllable because they can be expressed as $\delta\lambda_c = P\delta q_c$ and thus can be realized acting on the joints, compensable because the corresponding object displacement $\delta u_c = V\delta q_c$ belongs to the rigid body motion subspace and thus can be recovered with a suitable compensating control action.

It is worth underlying that the existence of the compensating controller is guaranteed by the fact that the rigid object motions in the column space of $\Gamma_{uc}$ and the controllable internal forces in the column space of $E$ can be jointly and independently controlled acting on the reference value of the joint variables as proved in [14].

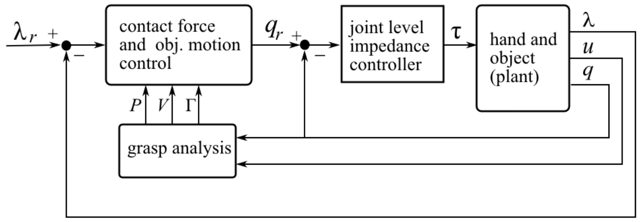


Fig. 2. Block diagram of the internal force and object motion control. The inner loop controls finger joint displacement, while the outer one seeks to control the internal forces to the reference value $\lambda_r$ without moving the object.

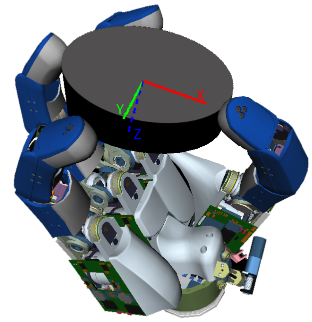

Fig. 3. Robotic hand and grasped object in the initial configuration.

The internal force controller corresponding to no motion of the object consists of two components. The first $\delta q_f$ sets joint reference to track the desired internal forces $\delta\lambda_c$ that belongs to the controllable and compensable subspace. The internal force controller alone generates an undesired effect which is the displacement of the object position in the subspace of the rigid-body object motions which can be compensated by an additional variation of joint references $\delta q_c$. The internal force controller with compensated motion is

$$\delta q_r = \delta q_f + \delta q_c \tag{9}$$

where

$$\delta q_f = P^{\#}\delta\lambda_c \tag{10}$$

$$\delta q_c = -\Gamma_{qc}\Gamma_{uc}^{\#} V \delta q_f \tag{11}$$

This control strategy allows to change the internal forces without affecting the motion of the grasped object.

The design of the object motion-decoupled control of internal forces has been performed in a quasi-static setting. We will validate the approach in a numerical experiment considering the hand and object dynamics.

The block diagram of the proposed controller is reported in Fig. 2. An external control loop implements the object motion-decoupled control of internal forces in (9). The reference for the internal force vector $\lambda_r$ is compared to the current contact forces $\lambda$ and the error

$$\delta\lambda_c = \lambda_r - \lambda$$

drives the external force controller which integrates the current value of the joint reference variable with the quasi-static joint reference displacement given by the decoupling control in (9).

The robotic hand joints are controlled with a joint-level impedance controller. The reference inputs are the reference joint rotation angles $q_r$ and their angular velocities $\dot{q}_r$. The joint-level impedance controller can be represented as a mechanical stiffness for the proportional term and a viscous damping for the derivative term. The proportional coefficient matrix corresponds to the mechanical stiffness $K_q$ in Section II. The joint motor torques, expressed with respect to the joint rotation axis, are given by

$$\tau = K_q(q_r - q) + B_q(\dot{q}_r - \dot{q}) + g(q)$$

where the stiffness matrix $B_q$ is the damping matrix and is chosen as a function of the stiffness matrix and the hand inertia matrix, to get a sufficiently damped system response, and $g(q)$ is the gravity vector of the hand links.

## IV. Numerical Experiments

### A. Hand description

In this section some experiments performed with a realistic numerical model of hand dynamics to test the object motion-decoupled control of internal forces proposed in Section III are described. The robotic hand used in the numerical experiments is the multifingered anthropomorphic DLR Hand II [7]. This device is composed of four identical modular fingers, each of them with 3 DoFs, so the hand has overall 12 DoFs. Each joint, except the distal ones, is provided with its own motor. The kinematic structure of each finger is anthropomorph–inspired: the metacarpo - phalangeal joint of each finger, the joint connecting the finger to the hand palm, has 2 DoFs, while the proximal interphalangeal joint has a single DoF. The distal interphalangeal finger rotation is coupled with the proximal one, with a gear ratio 1:1. Each finger consists of three identical modular parts and has three different type of sensors: each joint is provided with a torque sensor and a position sensor.

We consider an initial configuration where the object is grasped by the hand, the contacts are placed at the four fingertips and the initial contact forces $\lambda(0) = 0$. Henceforth we will consider the variations of the contact forces with respect to the initial condition. The hand initial configuration, which is chosen such that the system is initially in equilibrium, is shown in Fig. 3. The approaching phase in not considered in this numerical experiment, we suppose that the hand in the initial configuration is grasping the object. During the numerical experiment, the reference contact forces $\lambda_r$ are varied and the actual contact forces and object displacement are analyzed. In particular the effect of the compensating term $\delta q_c$ is investigated.

The object is defined through its contact points and normals at the contact points. The four contact points are supposed to be on the four fingertips of the hand. For simplicity we choose an object frame $OXYZ$ attached to the geometric center of the fingertip positions (see Fig. 3). The $X$ and $Y$ axes are chosen on the plane spanned by the directions connecting the direction through the thumb and middle fingertips to those connecting the index with the ring fingertips, while the $Z$ axis is orthogonal to such plane [17]. The unit normal vectors at the contact points are defined as the directions connecting the contact points to the object center above defined. For this numerical experiment the contacts were modeled as point contacts with friction (PCWF) [16].

By assuming a suitable selection of $y$, each contact force vector lies within the friction cone and has three components only. The dimension of the overall contact force vector is $\lambda \in \Re^{12}$. The dimensions of the grasp matrix are $G \in \Re^{6\times 12}$, while the dimensions of the hand Jacobian matrix are $J \in \Re^{12\times 12}$. No hand kinematic singularities[2] occurred during the numerical experiments. The contact stiffness matrix $K_s$ is diagonal, but the stiffness values are not the same for each finger. The contact stiffness matrix is chosen to obtain an asymmetric stiffness distribution, to highlight the effect on the object motion trajectory due to an uncompensated internal force controller, and to validate the effect of the proposed control motion-decoupled controller. The thumb stiffness has been chosen lower than the other fingers' ones, i.e. $K_s = \text{diag}[K_{s,t}, K_{s,f}]$, where $K_{s,t} = k_{s,t}I_3$, and $K_{s,t} = k_{s,f}I_9$ with $k_{s,t} = 50$ N/m and $k_{s,f} = 100$ N/m respectively, while $I_3 \in \Re^{3\times 3}$ and $I_9 \in \Re^{9\times 9}$ are identity matrices. In the numerical experiments, a viscous damping term was added, such that the contact forces are computed as

$$\lambda = K_s(c^h - c^o) + B_s(\dot{c}^h - \dot{c}^o)$$

with the damping matrix $B_s = b_s I_{12}$, in which $b_s = 5$ Ns/m. Also the joint stiffness matrix $K_q$ is diagonal, in this case different values were adopted for each joint: $K_q = \text{diag}[k_{q,1}, \cdots, k_{q,12}]$, with $k_{q,i} = 9$Nm/rad for the metacarpo - phalangeal joints, while $k_{q,i} = 4.5$ Nm/rad for the proximal-interphalangeal joints. The elements of the joint impedance control damping matrix have been chosen proportional to the stiffness ones. The geometric terms are not considered in these numerical experiments. Internal force subspace is six–dimensional, i.e. $E \in \Re^{12\times 6}$ and rigid body motion subspace is 6–dimensional $\Gamma \in \Re^{18\times 6}$.

A realistic model is used to simulate dynamics of the DLR hand II [13]. The grasped object is modelled as a rigid body subject to a set of contact forces. Its dynamics is described by the differential equation system in [13]. The contact force vector is simulated according to a compliant model taking into account the fingertip contact stiffness.

### B. Experiments

Several experiments were performed to validate the effectiveness of the proposed object motion-decoupled control of internal forces.Each experiment is composed of two parts: in the first oneonly the term that allows to control internal force error, without object motion compensation, was considered, i.e. $\delta q_r = \delta q_f$, in the second one both the contact force and the object displacement were controlled according to the control law defined in (11). The time of the numerical experiment was 20s, with an integration routine with constant step size of 0.001s. Some tests were performed with smaller step sizes, but the results did not change significantly. The reference contact force $\lambda = \lambda_0$ was set constant.

Fig. 4 shows the contact force variations with respect to the the initial value $\lambda_0$ at the fingertips during the numerical experiments, for each finger, compared with the reference force. Fig. 4 shows the results obtained when both the contact force and the object motion are controlled. The results obtained without object motion compensation look very similar to those shown in Fig. 4, even if the steady state error is smaller, as we can see observing the numerical results summarized in in Table I. As it can be seen from the plots, the reference force signal is followed with a stable dynamics and the steady state errors, even if larger than the non-compensated case, are acceptably small, the mean value, in the considered simulation, is about 2%.

[2]The finger has only one (boundary) singularity, that is the strechted out configuration.

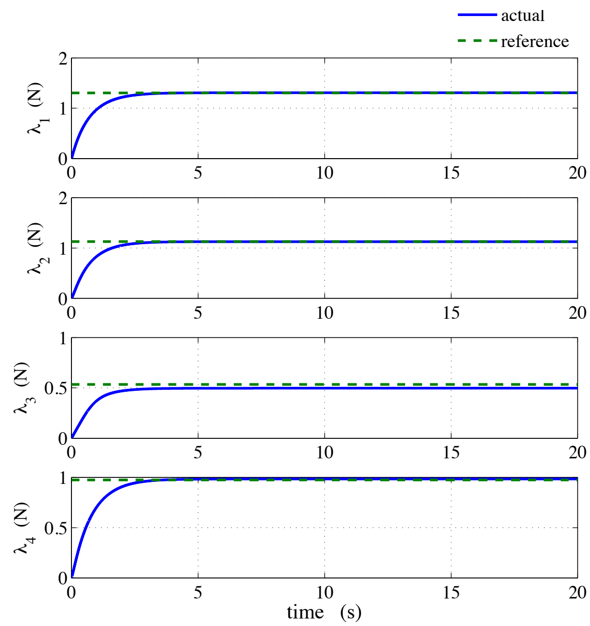


Fig. 4. Norms of the contact forces at the four fingertips during the numerical experiment, obtained with the object motion-decoupled control of internal forces defined in eq. (11). Each diagram represents, for each finger, the actual (solid line) and reference (dashed line) contact force norm.

| Motion compensation | No | Yes |
|---|---|---|
| object displacement (mm) | 6.0 | 1.8 |
| object displacement $x$ (mm) | 1.7 | 0.45 |
| object displacement $y$ (mm) | 2.1 | 0.57 |
| object displacement $z$ (mm) | 5.2 | -1.7 |
| mean force error (N) | $2.08 \times 10^{-5}$ | 0.0132 |
| mean force error (%) | 0.0031 | 2.12 |

TABLE I

CONTACT FORCE STEADY STATE ERRORS AND OBJECT DISPLACEMENT WITH AND WITHOUT OBJECT MOTION COMPENSATION.

Fig. 5 shows the moduli of the object displacement for the two numerical experiments. The steady state displacement components and the amplitudes obtained in the experiments are summarized in Table I. The final object displacement amplitude is 6 mm without the compensating term and 1.8 mm with the object displacement compensation. The results clearly show the effect of compensation of object motion in contact force control, that allows to significantly reduce the final displacement.

Finally, Fig. 6 illustrates the numerical result of the hand model viewer software: in the left column the initial hand and object (hockey puck) are shown, while in the left one the final configurations obtained without the proposed controller and with it are shown. The initial object configuration is superimposed (black disks) to the new one. As it can be seen, without the proposed controller, the object visibly moves while the contact forces are changing, on the contrary,

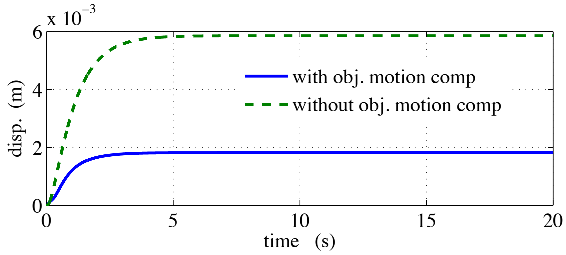


Fig. 5. Displacement of the object center (amplitude) during the numerical experiment, obtained controlling only the contact forces, without compensating the object motion (dashed line), and with the object motion-decoupled control of internal forces defined in eq. (11) (solid line).

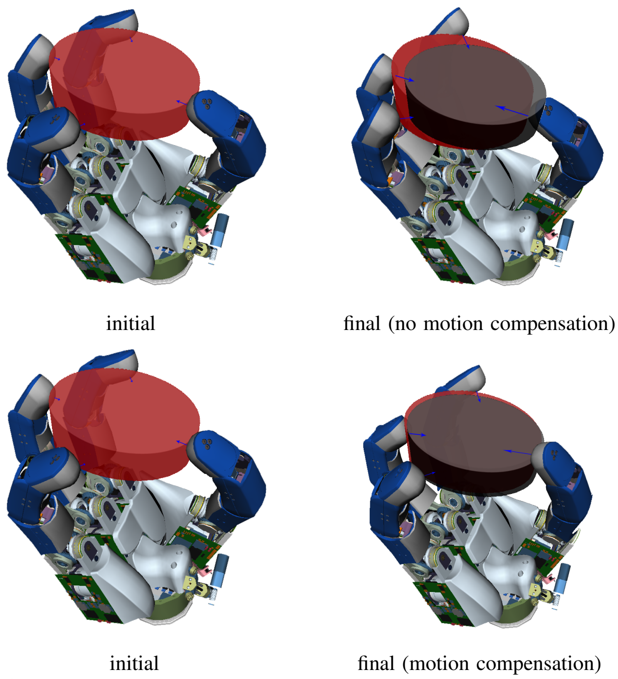


Fig. 6. Robotic hand, object displacements and contact forces obtained in the experiments, first row: controlling only the contact forces, without compensating the object motion; second row: with the object motion-decoupled control of internal forces defined in eq. (11), that compensates the object motion. The left figures show the initial hand and object configuration, the right ones the final.

introducing the motion compensation term, the object motion sensibly decreases.

## V. Conclusions

The coupling between internal force control and object motion control is crucial in compliant multifingered hands. Intuitively, when compliance is significant, it happens that a variation in the contact forces applied on the grasped object causes the object trajectory to deviate from the planned path with consequent performance degradation. This paper studied the structural conditions to design an internal force controller decoupled from object motions. The analysis was constructive and a controller of internal forces was proposed, starting from a quasi static grasp analysis. We referred to this controller as object motion-decoupled control of internal forces.

The force controller was then successfully tested on a realistic model of the DLR Hand II. The results of the numerical tests demonstrated that the proposed object motion-decoupled control of internal forces, derived with a quasi static analysis, can effectively produce a significant reduction on the object displacement also in dynamic conditions, when the reference contact force are varied: the final object displacement reduction obtained introducing the compensating term in the control system was significantly lower than those obtained simply controlling the squeezing forces.

Future developments of this work will include the analysis of the external wrench contribution to the object dynamics and the effect of the geometrical terms on the motion-decoupled control of internal forces.

## VI. Acknowledgements

This work has been partially supported by the European Commission with the Collaborative Project no. 248587, “THE Hand Embodied”, within the FP7-ICT- 2009-4-2-1 program “Cognitive Systems and Robotics” and the Collaborative EU-Project “Hands.dvi” in the context of ECHORD (European Clearing House for Open Robotics Development).

## References

[1] A. Albu-Schäffer, O. Eiberger, M. Grebenstein, S. Haddadin, C. Ott, T. Wimböck, S. Wolf, and G. Hirzinger. Soft robotics. *IEEE Robotics & Automation Magazine*, 15(3), September 2008.

[2] L. Biagiotti, P. Tiezzi, G. Vassura, and C. Melchiorri. Modelling and controlling the compliance of a robotic hand with soft finger-pads. In Federico Barbagli, Domenico Prattichizzo, and Kenneth Salisbury, editors, *Multi-point Interaction with Real and Virtual Objects*, volume 18 of *Springer Tracts in Advanced Robotics*, pages 55–73. Springer Berlin / Heidelberg, 2005.

[3] A. Bicchi. Force distribution in multiple whole-limb manipulation. In *Proc. IEEE Int. Conf. Robotics and Automation*, 1993.

[4] A. Bicchi. On the problem of decomposing grasp and manipulation forces in multiple whole-limb manipulation. *Int. Journal of Robotics and Autonomous Systems*, 13, 1994.

[5] A. Bicchi and D. Prattichizzo. Manipulability of cooperating robots with unactuated joints and closed-chain mechanisms. *IEEE Trans. Robotics and Automation*, 16(4), 2000.

[6] L. Birglen. From flapping wings to underactuated fingers and beyond: a broad look to self-adaptive mechanisms. *Mechanical Sciences*, 1(1):5–12, 2010.

[7] J. Butterfaß, M. Grebenstein, and H. Liu. DLR-Hand II: next generation of a dextrous robot hand. In *Proceedings ICRA. IEEE International Conference on Robotics and Automation*, volume 1, pages 109 – 114, 2001.

[8] M. Ciocarlie and P. Allen. A design and analysis tool for underactuated compliant hands. In *Intelligent Robots and Systems, 2009. IROS 2009. IEEE/RSJ International Conference on*, pages 5234 –5239, oct. 2009.

[9] M.R. Cutkosky and I. Kao. Computing and controlling compliance of a robotic hand. *IEEE Transactions on Robotics and Automation*, 5(2), 1989.

[10] A.M. Dollar and R.D. Howe. Simple, robust autonomous grasping in unstructured environments. In *Robotics and Automation, 2007 IEEE International Conference on*, 2007.

[11] T. Laliberté and C. Gosselin. Simulation and design of underactuated mechanical hands. *Mechanism and Machine Theory*, 33(1-2):39 – 57, 1998.

[12] M. Malvezzi and D. Prattichizzo. Internal force control with no object motion in compliant robotic grasps. In *IEEE/RSJ International Conference on Intelligent Robots and Systems*, 2011.

[13] R. M. Murray, Z. Li, and S. Sastry. *A Mathematical Introduction to Robotic Manipulation*. CRC Press, Boca Raton, FL, 1994.

[14] D. Prattichizzo and A. Bicchi. Consistent specification of manipulation tasks for defective mechanical systems. *ASME Jour. Dynam. Systems, Measurement, and Control*, 119, 1997.

[15] D. Prattichizzo and A. Bicchi. Dynamic analysis of mobility and graspability of general manipulation systems. *IEEE Trans. on Robotics and Automation*, 14(2):241–258, 1998.

[16] D. Prattichizzo and J. Trinkle. *Grasping*. Handbook on Robotics, Springer, 2008.

[17] T. Wimböck, C. Ott, and G. Hirzinger. Analysis and experimental evaluation of the intrinsically passive controller (IPC) for multifingered hands. In *IEEE International Conference on Robotics and Automation, ICRA*, pages 278 – 284, 2008.